12. E. Kausel and R. Peek. Dynamic Loads in the Interior of a Layered Stratum: An Explicit Solution. Bulletin of the Seismological Society of America, Vol. 72, No. 5, Oct. 1982, pp. 1459-1481.
13. R.J. Apsel. Dynamic Green's Functions for Layered Media and Applications to Boundary-Value Problems. Ph.D. dissertation. University of California at San Diego, 1979.
14. F.E. Richart, Jr., J.R. Hall, Jr., and R.D. Woods. Vibrations of Soils and Foundations. Prentice-Hall, Inc., Englewood Cliffs, N.J., 1970.

Publication of this paper sponsored by Committee on Mechanics of Earth Masses and Layered Systems.

Dynamic Interpretation of Dynaflect and Falling Weight Deflectometer Tests

JOSE M. ROESSET and KO-YOUNG SHAO

ABSTRACT

The Dynaflect and the falling weight deflectometer are commonly used for nondestructive testing of pavements. In both cases a dynamic load is imparted, and the determination of the mechanical properties of the pavement, the base, and the subbase is normally performed by comparing the measured deflections at various points along the surface to results of static analyses that consider the subbase as a homogeneous, elastic half-space. In this paper, the displacements obtained from dynamic analyses are compared to those provided by conventional static programs when the subbase is a homogeneous soil stratum of finite depth resting on a much stiffer rocklike material and when the soil properties increase smoothly with depth, as is often the case. The results of these comparisons indicate that for certain ranges of depth to bedrock a static interpretation of the Dynaflect and falling weight deflectometer tests may lead to substantial errors. Situations in which these errors are important are more likely to be encountered with the Dynaflect than with the falling weight deflectometer.

The Dynaflect and the falling weight deflectometer are commonly used for nondestructive testing of pavements. The Dynaflect consists of a force generator and five geophones housed in a small trailer, which is towed by a light vehicle. The loading system consists of two counterrotating eccentric masses. The resulting vertical force varies harmonically with time. At a frequency of 8 Hz, a 1,000-lb peak-to-peak oscillating force and a base load of 1,000 lb are transmitted to the pavement through the loading wheels. The resulting deflection basin is measured by five geophones that are mounted on the trailer draw bar at 12-in. intervals. The positions of the geophones (ST1 through ST5) with respect to the wheels are shown schematically in Figure 1.

The falling weight deflectometer has a 330.7-lb (150-kg) weight mounted on a vertical shaft and housed in a compact trailer that can easily be towed by most conventional passenger cars. The weight is hydraulically lifted to a predetermined height (ranging from 0 to 15.7 in. or 0 to 400 mm). It is then dropped onto a rubber pad 11.8 in. (300 mm) thick, that helps to distribute the load uniformly over the loading area. The resulting load is a force impulse with a duration of approximately 30 msec and a peak magnitude ranging from 9 to 14,000 lbs (0 to 60 000 N) depending on the drop height. The peak force and maximum deflections at various points along the surface are measured by load cells and velocity transducers. The applied pressure is measured in kilopascals and the deflections in micrometers.

In the case of the Dynaflect the deflections measured at the various stations represent the amplitudes of the steady-state displacements at a given frequency (8 Hz). For the falling weight deflectometer they are the peak displacements under a transient-type excitation. In both cases the tests are dynamic in nature, but the interpretation of their results to estimate the elastic properties of the pavement, base, and subbase relies on static analyses. Furthermore, these analyses assume that the soil in the subbase is an elastic, homogeneous, and isotropic half-space. In many cases soil properties

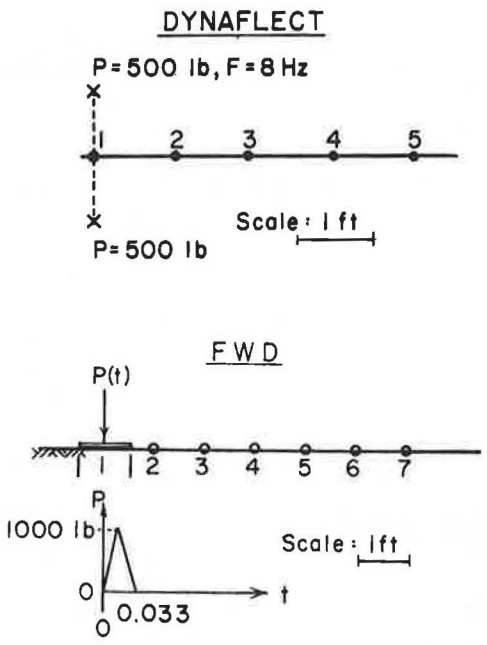

FIGURE 1 Geometric configuration of loads and stations for Dynaflect and falling weight deflectometer.

will vary with depth and the soil will be underlain at some depth by stiffer, rocklike material.

The purpose of this work is to determine the dynamic displacements at points along the surface of a pavement excited by forces simulating the excitation of the Dynaflect and the falling weight deflectometer. These displacements are compared for various depths to bedrock with those resulting from static analyses for the same soil profile and assuming an elastic half-space (the normal assumption). The dynamic deflection bulbs obtained from the analyses are then used as input for the standard backfiguring process to estimate the elastic moduli of the pavement, base, and subbase in order to assess the errors induced by neglecting dynamic effects.

FORMULATION

Consider a soil deposit that consists of horizontal layers. The mass density and the elastic moduli of the soil may change with depth, from layer to layer, but are assumed to be constant over each layer. For the present application the top layer would represent the pavement (assuming that it extends to infinity in both horizontal directions), the second layer would be the base, and the remaining layers would represent the soil of the subbase. An accurate solution would require consideration of the finite width of the pavement. Even so, for the purposes of this study, these simplifying assumptions should not be unreasonable. The determination of the response of this soil deposit to dynamic loads applied at the surface (or at any point within the soil mass) falls mathematically into the area of wave propagation theory.

The formulation of these problems always starts by considering steady-state harmonic forces and displacements at a given frequency. For a harmonic excitation, as caused by a vibrating machine rotating at a specified velocity (case of the Dynaflect), the solution at the corresponding frequency provides directly the desired results. For an arbitrary transient excitation (case of the falling weight deflectometer), the time history of the specified forces must be decomposed into different frequency components using a Fourier series, or more conveniently a Fourier transform. Results are then obtained for each term of the series (each frequency) and combined to obtain the time history of displacements (inverse Fourier transform).

For an isolated layer with uniform properties, the stresses and displacements along the top and bottom surfaces can be expanded in a double Fourier series (or Fourier transform) in the two horizontal directions for Cartesian coordinates, or in a Fourier series in the circumferential direction and a series of modified Bessel functions in the radial direction for cylindrical coordinates. For each term of these series, corresponding to a given wave number, there can be determined closed-form analytical expressions in the form of a transfer matrix relating amplitudes of stresses and displacements at the bottom surface to the corresponding quantities at the top (or vice versa). This approach [Thomson (1) and Haskell (2)] has served as the basis for most studies on wave propagation through layered media in the last 30 years. An alternative is to relate the stresses at both surfaces to the displacements, obtaining a dynamic stiffness matrix for the layer (3), which can be used and understood in much the same way as those in structural analysis. For a half-space, the stiffness matrix relates directly stresses and displacements at the top surface because the bottom surface is pushed to infinity. Assembling the stiffness matrices of the different layers, there can be obtained a stiffness matrix for the complete soil deposit, which relates forces per unit of area applied at the free surface, or the interfaces between the layers, to the displacements at the same elevations.

The terms of the transfer or stiffness matrices of each layer are transcendental functions (complex exponentials). In addition, results must be obtained for each term of the Fourier series decomposition (each wave number), then combined, normally by numerical integration, to obtain the solution for a specified load distribution. On the other hand, the thickness of the layers is controlled only by physical considerations and the assumption of uniform properties. This makes the procedure particularly convenient when dealing with a homogeneous half-space or a small number of layers but extremely expensive when a large number of layers are needed to reproduce properly the variation of soil properties with depth. Formulations along these lines have been implemented by Gazetas (4) in Cartesian coordinates and by Apsel (5) in cylindrical coordinates.

When the layers are extremely thin, the transcendental functions representing the variation of displacements with depth can be approximated over each layer by a straight line (or higher order polynomial expansions). The solution (displacements and stresses) is then expressed in terms of the exact analytical expressions in the two horizontal (or radial and circumferential) directions and in terms of simpler polynomial expansions in the vertical direction (as in a finite element formulation). This approximation leads to much simpler algebraic expressions for the terms of the transfer or stiffness matrices of the layers. In addition, when the soil is underlain by a much stiffer, rocklike material, which can be considered rigid, it is possible to determine the wave numbers (eigenvalues) and the mode shapes (eigenvectors) of the waves propagating through the soil deposit by solving an algebraic eigenvalue problem (6,7). Expressing the solution in terms of these mode shapes (eigenfunction expansion), Kausel (8) was able to obtain explicit solutions for the displacements caused by harmonic dy-

namic loads in a layered soil deposit. Kausel's formulation is particularly efficient from the point of view of computation, but the layers must be sufficiently thin to reproduce accurately the variation of the displacements with depth with a piecewise linear approximation.

Because the purpose of this work was to investigate the effects of depth to bedrock and variation of soil properties with depth on the dynamic response of a pavement, it was decided to use Kausel's formulation. The formulation was implemented in a computer program and the results were compared with those published by Kausel (8) with excellent agreement. Because of the discrete nature of the formulation, before it is applied, an appropriate mesh size (thickness of the sublayers) to guarantee an accurate solution must be determined.

Studies were conducted first for static loads (zero frequency), a homogeneous soil deposit of finite depth, and a vertical load on the surface uniformly distributed over a circular area with a radius (r_o) of 1 in. (simulating the loading in the Dynaflect) or 6 in. (approximate dimensions of the loading plate of the falling weight deflectometer). The properties of the soil deposit are shown in Figure 1. This represents another approximation because the load distribution for the Dynaflect will be more nearly elliptical. This simplification appears to be justified for the purposes of this study. A model with all layers of the same thickness was initially considered. Figure 2 shows typical results for a deposit 40 ft deep. The displacements at the center of the loaded area and at distances (d) of 2 and 4 ft from this point are divided by the exact solution and plotted versus the inverse of the number of layers. Ten layers correspond, therefore, to a layer thickness of 4 ft. It can be seen from this figure that excellent results are obtained at distances of 2 and 4 ft even with the coarser mesh (10 layers). The error for a distance of 2 ft is slightly larger for the small loaded area (radius of 1 in.), but it is only 2 percent with the coarse mesh. Results at the center of the loaded area are, on the other hand, extremely poor even when taking

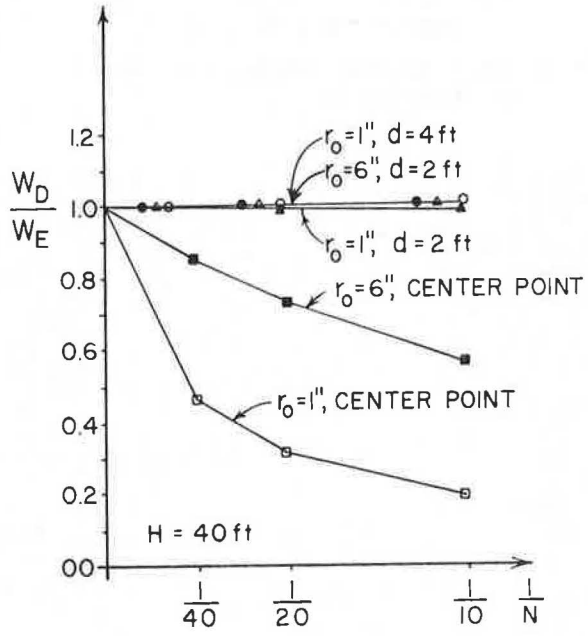

FIGURE 2 Variation of displacements with number of layers at H = 40 ft, W_E = exact solution.

40 layers (thickness of 1 ft for each layer), and they are much worse for the small loaded area. This indicates that for static loads the thickness of the layers has to decrease with decreasing distance between the load and the point where displacements are computed.

Figure 3 shows the ratio (w_H/w_∞) where w_H is the displacement for a stratum of depth H and w_∞ is the displacement for a half-space. The displacements are computed at the center of the loaded area and at distances (d) of 2 and 4 ft. They are plotted versus the inverse of the stratum thickness to better illustrate the convergence rate. The results indicate that the displacement is nearly inversely proportional to H. It is interesting to note that at the center of the loaded area the displacements for a stratum with a depth of only 8 ft are already within 1 percent of the results for a half-space with a radius of 1 in. and within 5 percent for the 6-in. radius. The depth needed to reproduce a half-space increases clearly with increasing distance between the load and the point where displacements are computed. This suggests also that close to the load the static displacements are affected only by the soil properties near the surface, whereas for increasing distances the soil properties at larger depths will influence the results more significantly.

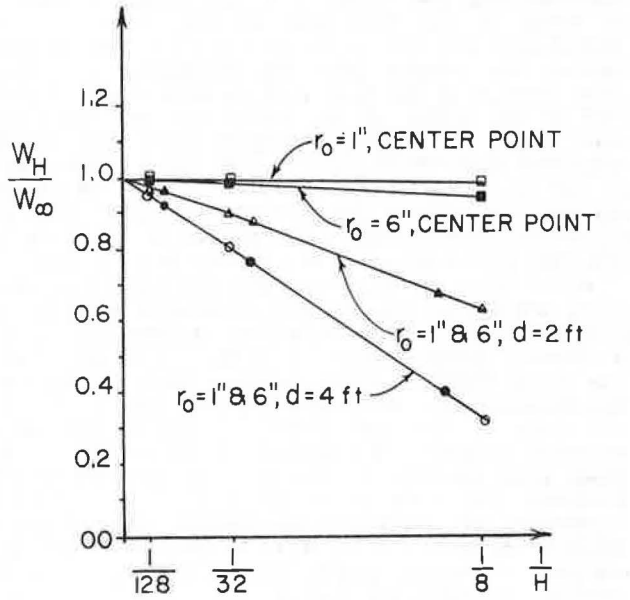

FIGURE 3 Variation of displacements with depth to bedrock.

On the basis of the observations from these two series of studies, it was decided that an improvement in the accuracy and the economy of the computations could be obtained by taking thin sublayers near the surface and gradually increasing their thickness with depth. The distance from the center of the loaded area to the point where the displacements are computed was designated D, and a rule was derived to automatically generate a desired mesh. According to this rule the first D ft are divided into 2N sublayers of equal thickness, and the next D ft are divided into N sublayers. N sublayers are then used for the following 2D ft, the next 4D ft, and so forth. When results are desired under the loaded area the distance D is replaced by the radius of the loaded area. For a nonhomogeneous soil deposit (such as a pavement), the thickness of each

TABLE 1 Displacements for Different Meshes (10^{-8} ft)

Radius of Disk (in.)	Center Point				d = 2 ft				d = 4 ft			
	H (ft)	Fine	Standard	Coarse	H (ft)	Fine	Standard	Coarse	H (ft)	Fine	Standard	Coarse
6					2							
	8	35.27	34.88	33.48	8	2.971	2.970	2.909	8	0.7609	0.7664	0.7613
	32	36.58	36.20	34.78	32	4.237	4.230	4.148	32	1.887	1.884	1.847
	128	36.92	36.53	35.10	128	4.566	4.557	4.472	128	2.214	2.209	2.168
1	5.33	219.6	217.3	208.7	8	2.932	2.930	2.873	8	0.7553	0.7607	0.7560
	21.33	221.6	219.2	210.7	32	4.200	4.192	4.113	32	1.883	1.879	1.843
	85.33	222.1	219.8	211.2	128	4.529	4.519	4.437	128	2.209	2.205	2.164

sublayer is the smaller of the value suggested by the rule or the actual physical dimension of the layer. When the physical thickness controls, the mesh generated according to the rule is subdivided automatically to accommodate this criterion. Finally, when the results are obtained simultaneously at various points, the smallest D (or the radius of the loaded area) controls.

This rule was used to construct meshes with values of N equal to 4, 2, and 1. These will be referred to as fine, standard, and coarse mesh, respectively. Results were then obtained for a homogeneous soil deposit with a Young's modulus (E) of 20 ksi and a Poisson's ratio of 0.4. The displacements obtained with the coarse mesh are within 5 percent of those of the fine mesh at the center of the loaded area and improve in accuracy for greater distances. The results with the standard mesh differ from those with the fine mesh by less than 1.5 percent at the center of the loaded area and are again even closer for greater distances (Table 1). It was concluded from these results that the standard mesh should be sufficiently accurate for most practical applications. Given the various approximations and uncertainties involved in all phases of these analyses, the coarse mesh may be adequate in many cases.

Using these three meshes and the same soil profile, parametric studies were conducted next for a dynamic excitation and different frequencies. It is a commonly accepted rule of thumb, in dynamic studies using finite element models, that the size of the elements must be of the order of one-quarter to one-sixth of the wavelength to obtain reasonably accurate results. The wavelength is equal to the shear wave velocity of the material divided by the frequency for shear waves and the P wave velocity divided by the frequency for compressional or dilatational waves. If E is Young's modulus of the material, υ its Poisson's ratio, and ρ its mass density, the shear modulus is

$$G = E/2(1 + \upsilon) \quad (1)$$

and the constrained modulus is

$$\lambda + 2G = E(1 - \upsilon)/(1 + \upsilon)(1 - 2\upsilon) \quad (2)$$

The shear wave velocity (v_S) is then given by

$$v_S^2 = G/\rho \quad (3)$$

and the P wave velocity is

$$v_S^2 = (\lambda + 2G)/\rho = v^2\, 2(1 - \upsilon)/(1 - 2\upsilon) \quad (4)$$

The Rayleigh wave velocity, associated with surface waves generated by a surface loading, is only slightly smaller than the shear wave velocity (v_S).

Figure 4 shows the amplitude of the steady-state displacements obtained with the fine and standard meshes at a point 5 ft from the center of the loaded area. The displacements are plotted versus a dimensionless frequency. A value of the dimensionless frequency of 1 corresponds to an actual frequency of 16 Hz and a wavelength of approximately 32 ft. The maximum layer thickness, at the bottom of the soil profile, in the standard mesh is 8 ft and in the fine mesh 4 ft. It can be seen that the results are in good agreement up to a dimensionless frequency of about 1, corresponding to a wavelength equal to four times the maximum layer thickness of the standard mesh. For higher frequencies the results of the standard mesh exhibit a series of sharp peaks that are not present in the more refined solution. Figure 5 shows similar results using the fine mesh and a mesh with twice the number of layers (each layer half the thickness of those in the fine mesh). The two solutions are almost identical up to a dimensionless frequency of about 2, corresponding to a wavelength equal to four times the maximum layer thickness of the fine mesh. In both cases the agreement is even better when the displacements at closer distances are considered. The distances involved in the Dynaflect and falling weight deflectometer tests are smaller than or equal to 6 ft.

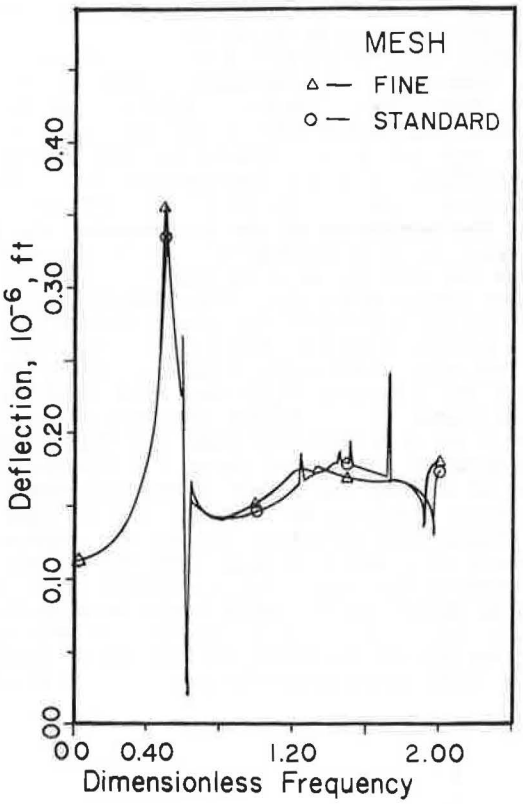

FIGURE 4 Amplitude of displacements at Point 7, fine and standard meshes.

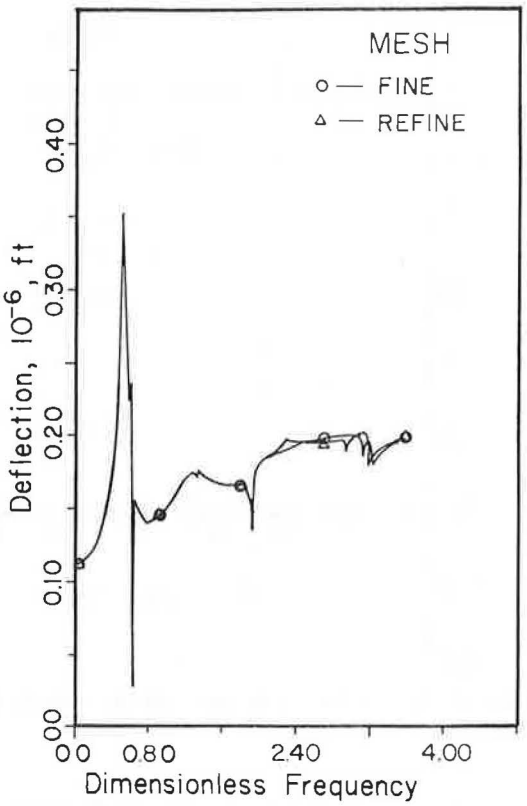

FIGURE 5 Amplitude of displacements at Point 7, fine and refined meshes.

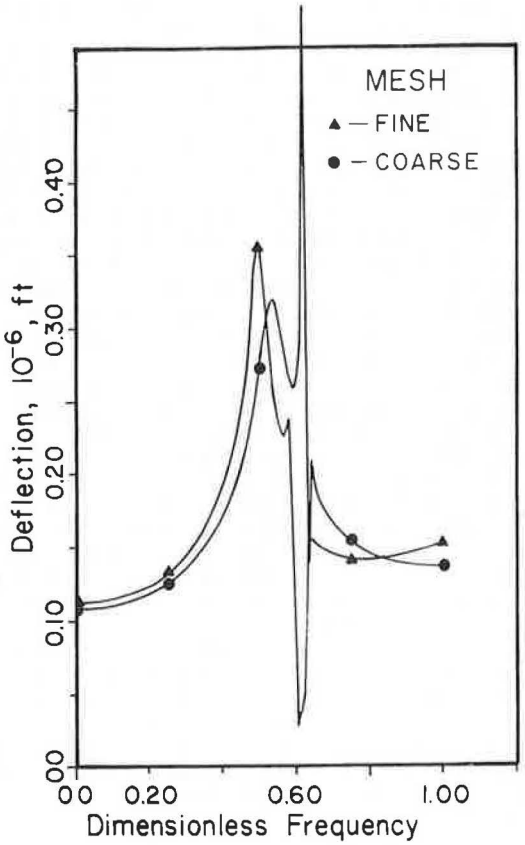

FIGURE 6 Amplitude of displacements at Point 7, fine and coarse meshes.

Figure 6 shows the results using the fine and coarse meshes. The differences in this case are of the same order of magnitude as those reported for static loads in the low-frequency range, but they become much more pronounced for dimensionless frequencies greater than 0.4 (wavelengths less than 5 times the maximum layer thickness).

These results appear to confirm the validity of the rule of thumb commonly used in practice. The standard mesh will provide good results for the dynamic case as long as the wavelengths are longer than four times the maximum thickness of any layer. For higher frequencies the mesh must be modified to satisfy this additional constraint (reducing the thickness of the bottom layers).

SIMULATION OF DYNAFLECT TESTS

A pavement system was selected to evaluate the importance of dynamic effects on the results of the Dynaflect tests (Figure 7). The pavement has a thickness of 2.5 in. and a Young's modulus of 200 ksi; the base has a thickness of 15 in. and a modulus of 78.5 ksi. The soil of the subbase was considered homogeneous with a Young's modulus of 29 ksi and with a modulus starting with this value at the top and increasing with depth. Different depths to bedrock were used in the range from 10 to 110 ft. Displacements were computed at the points corresponding to the stations of the Dynaflect for a static load and for a frequency of 8 Hz.

Figure 8 shows the variation of the static displacements with depth to bedrock at the five stations. Figure 9 shows the corresponding results for a frequency of 8 Hz, typical of Dynaflect tests.

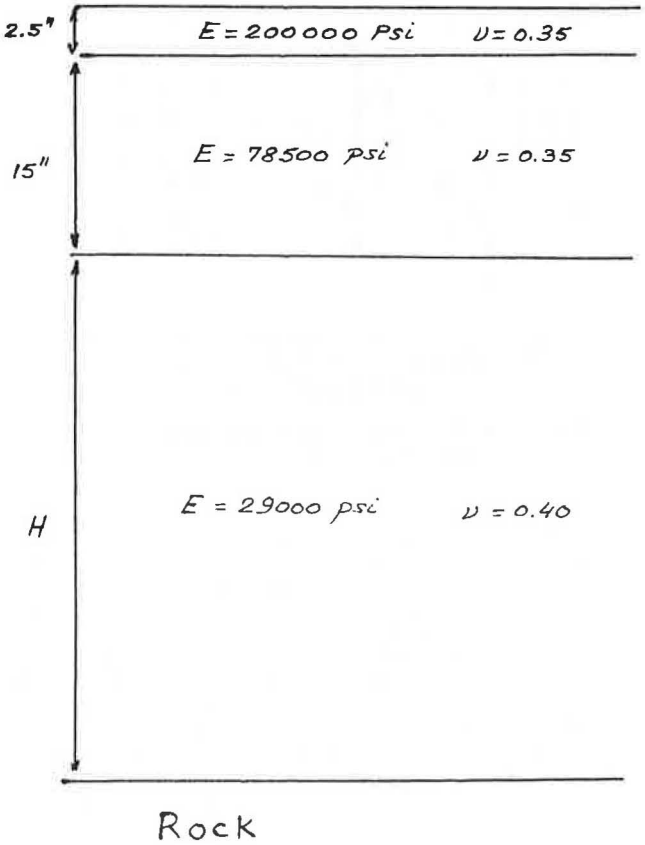

FIGURE 7 Profile of pavement used for studies.

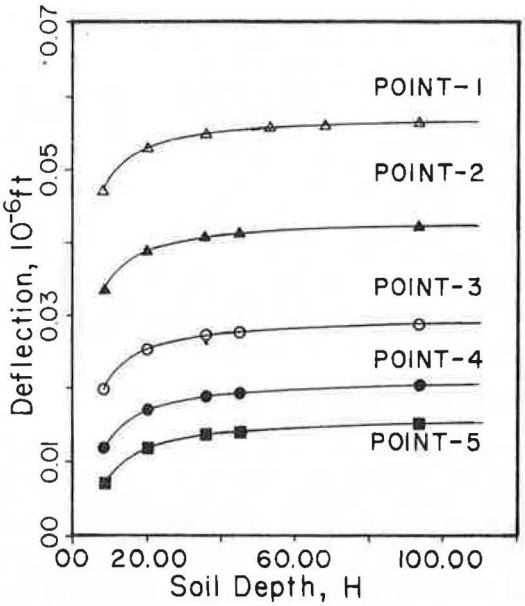

FIGURE 8 Variation of static displacements with depth to bedrock—Dynaflect.

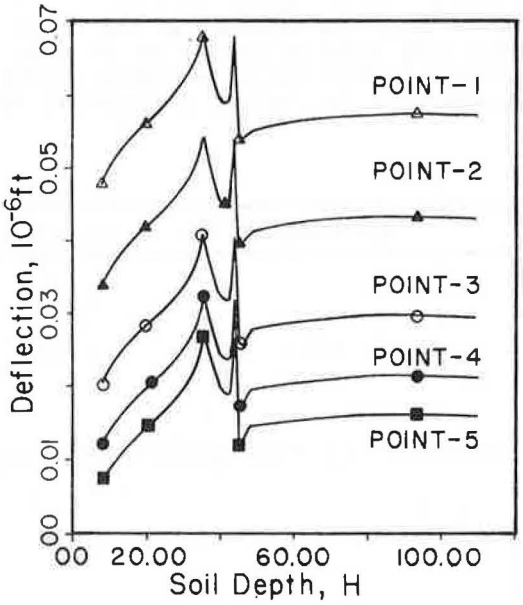

FIGURE 9 Variation of dynamic displacements with depth to bedrock—Dynaflect.

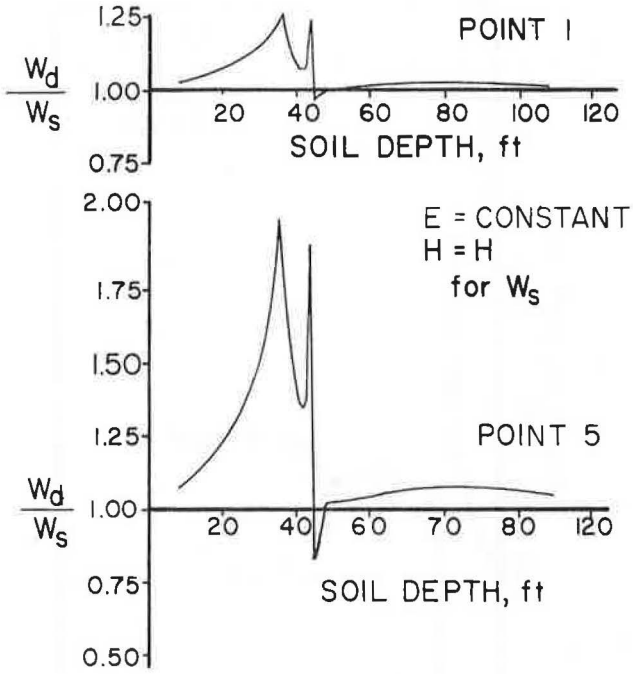

FIGURE 10 Ratio of dynamic to static deflections, Points 1 and 5—Dynaflect.

Figure 10 shows, finally, the ratio of the dynamic to the static displacements at Points 1 (between two wheels) and 5 (farthest from the loads). As the depth to bedrock increases so does the ratio of dynamic to static deflections, reaching a peak for a depth of approximately 35 ft and a second, much sharper peak for a depth of about 42 ft and exhibiting a sharp valley immediately after. As the depth to bedrock continues to increase the ratio appears to tend to 1 from above. Additional studies assuming 2 and 3 percent internal damping in the soil indicated that the first peak was only slightly affected by the existence of a small amount of material damping (which can always be expected) but that the second peak and the following trough disappeared almost entirely. The range of depths over which there is a substantial dynamic amplification of the deflections is closely associated with the depths for which a frequency of 8 Hz represents the natural frequencies of the soil deposit in shear and dilatation. These would be 20 and 48 ft, respectively.

Because the elastic properties of the pavement, base, and subbase are normally determined by comparing the measured deflections to those resulting from static analyses assuming that the subbase is an elastic half-space, it is perhaps more interesting to compare the dynamic results to the static deflections for an infinite depth to bedrock. The ratio of these deflections for Points 1 and 5 is shown in Figure 11. These results indicate that for shallow depths to bedrock (less than 20 or 25 ft) the dynamic deflections are smaller than the static deflections for a half-space (although they are larger than the static deflections for the same soil profile with a finite depth). For a range of depths of from 25 to 40 ft the dynamic results are larger than the static ones because the dynamic amplification is more pronounced as the distance to the load increases. For depths greater than 50 or 60 ft the ratio of dynamic to static displacements is close to 1. It is thus for depths to bedrock of less than 40 ft that the errors committed by the present interpretation procedures can be most serious for this particular profile. (Greater depths would be significant if the soil of the subbase were stiffer than the one selected for this study.)

Determination of the characteristics of the profile from the measured deflections falls into the general category of system identification problems (sometimes referred to as the inverse problem). Because only five deflections are available, it is often assumed that the thickness of the pavement and the base are known and that the only unknowns are the moduli of elasticity. These moduli are normally estimated by a trial and error procedure, assuming a set of values, computing the corresponding static deflections, comparing them to the measured values, and iterating until the differences are smaller than

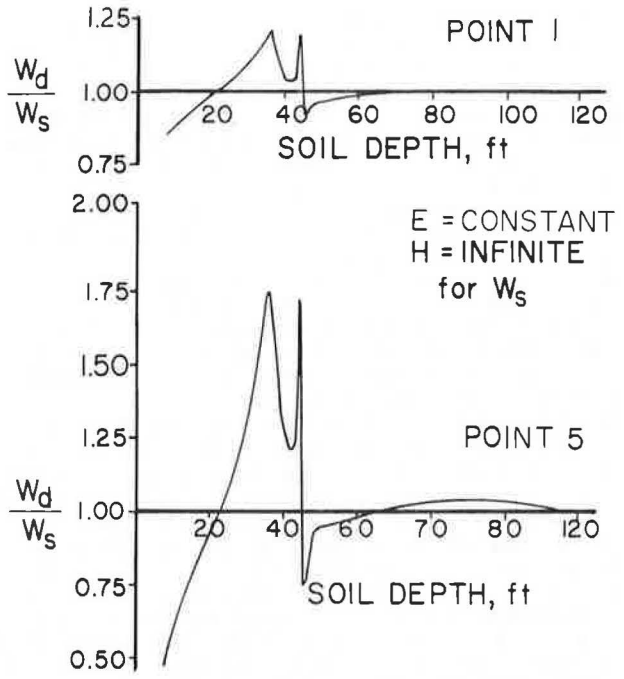

FIGURE 11 Ratio of dynamic to static (H = ∞) displacements, Points 1 and 5—Dynaflect.

an acceptable tolerance. Unfortunately, uniqueness of the solution cannot be guaranteed and different sets of elastic moduli can produce results that are within the specified tolerance.

To get a better feeling for the significance of the difference between static and dynamic displacements, the deflection bulbs computed for depths to bedrock of 10, 20, 35, and 110 ft were used as input to the identification procedure. The exact values of the elastic moduli were used as initial guesses and a gradient search technique was used in an attempt to converge to an optimum match using the computer program BASSD2 (9). The results of these studies are given in Table 2. Listed in the table are the computed deflections, the estimated values of the elastic moduli, and the errors in these moduli. It can be seen that for a depth to bedrock of only 10 ft the stiffness of the subbase is badly overestimated, whereas the modulus of elasticity of the base as well as the modulus of the pavement are underestimated. This occurs because the dynamic and finite layer effects are more pronounced for the farthest stations, the deflections of which are heavily influenced by the soil properties at greater depths. For a depth to bedrock of 20 ft the properties of the base and the soil are accurately determined, but the modulus of the pavement is badly overestimated. For a depth of 35 ft the moduli of the pavement and the base are both overestimated and the stiffness of the subbase is underestimated. This situation is the reverse of that encountered for a depth of 10 ft. When the depth of bedrock is 110 ft the results are more reasonable although the estimated modulus of the pavement is still 24 percent too high.

It is important to keep in mind that these results are not unique and that another person might obtain different values of the moduli with the same quality of fit. Even so, it is believed that the results illustrate reasonably well the type of errors and the variation in estimated properties that can be expected.

The same series of studies was conducted assuming that the soil properties increased gradually with depth. Figure 12 shows the ratio of the dynamic deflections for the soil profile with bedrock at a finite depth to the static deflections assuming that the subbase is homogeneous and extends to infinity. Notice that in this case the range of depths over which there is a substantial dynamic amplification is somewhat larger (from 20 to 60 ft approximately) because the subbase is effectively stiffer. An amplification effect is still apparent for a depth to bedrock of 110 ft whereas for the homogeneous soil the ratio of dynamic to static deflections is close to 1 for these depths.

SIMULATION OF FALLING WEIGHT DEFLECTOMETER TESTS

Because the loads applied by the falling weight deflectometer are transient in nature, it is necessary, to simulate the results of this test, to decompose the time history of the force into frequency components using the Fourier transform. Analyses must then be conducted for a large number of different frequencies to obtain the transfer functions of the deflections at each point (station). These transfer functions are then multiplied by the Fourier transform of the input and the resulting functions are converted back to time using the inverse Fourier transform. The final results are the time histories of the deflections at the various points. The complete analysis is clearly much more expensive than is the case of the Dynaflect where only one frequency is involved. Therefore the studies were

TABLE 2 Deflection Bulbs and Estimated Elastic Moduli for Homogeneous Subbase and Different Depths to Bedrock—Dynaflect

	H	Displacement (mils)					Young's Modulus	Error
	(ft)	Point 1	Point 2	Point 3	Point 4	Point 5	(lb/in^2)	(%)
Static	∞	0.70	0.52	0.36	0.26	0.20	200,000	
							78,500	
							29,000	
Dynamic	10	0.61	0.44	0.28	0.17	0.11	150,000	25.0
							30,000	61.8
							45,000	55.2
Dynamic	20	0.68	0.51	0.35	0.24	0.18	340,500	70.3
							78,000	0.6
							29,837	2.8
Dynamic	35	0.82	0.65	0.48	0.38	0.31	350,000	75.0
							98,500	25.5
							20,000	31.0
Dynamic	110	0.69	0.52	0.35	0.25	0.18	248,370	24.0
							78,500	0.0
							29,833	2.9

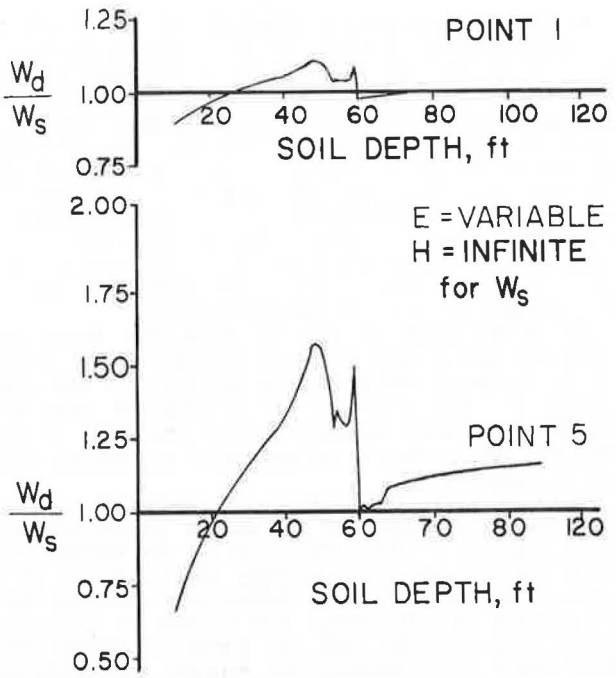

FIGURE 12 Ratio of dynamic to static (H = ∞) displacements, variable soil profile—Dynaflect.

limited to depths to bedrock of 10, 20, 40, and 80 ft.

The continuous Fourier transform involves an integral over time (direct transform) or frequency (inverse transform) extending from minus infinity or zero to infinity. In practice, however, a discrete transform, referred to as the fast Fourier transform, is used. In this case a finite number of points (power of 2) are selected to reproduce the function of time at equal time intervals (Δt). The total duration is $T = N\Delta t$ if N is the number of points. Notice that for an impulse-type load the values of the function will be nonzero for only a few points. The Fourier transform is then calculated at N/2 points with a frequency interval $\Delta f = 1/T$ and a maximum frequency (f_{max}) equal to $1/2\Delta t$. Proper selection of these parameters is important to guarantee the accuracy of the final results. A small time interval (Δt) is desirable to reproduce properly the time variation of the forcing function and to ensure that the peak response displacement is not missed. The total duration (T) should be several times larger than the actual duration of the load to ensure that spurious free vibration terms have attenuated; the appropriate value depends on the fundamental period of the system and the amount of damping (in the present case no internal damping is assumed for the soil and the only source of energy dissipation results from radiation or geometric spreading of the waves above the fundamental frequency of the soil stratum). The frequency increment Δf [fixed when the duration (T) has been selected] should be small to reproduce properly the transfer function, particularly if it exhibits some sharp peaks (typical of lightly damped systems). All these considerations point out the desirability of a small Δt and a large number of points N. It should be noticed, however, that as the number of points increases so do the cost of computation and the number of frequencies for which analyses must be conducted. As Δt decreases, the maximum frequency (f_{max}) increases. This requires more refined meshes and a larger number of layers because of the dynamic limitation on the thickness of the layers.

A number of preliminary studies were conducted to assess the values of Δt and N required to obtain reasonably accurate results. It was concluded from these studies that a value of N equal to 2,048 and a time interval of approximately 0.002 sec were appropriate for these applications. Figure 13 shows a typical transfer for the center of the loaded area and a depth to bedrock of 20 ft. (The transfer function is actually complex; the amplitude of the function is shown.) It can be seen that for frequencies larger than 20 Hz the function is relatively smooth without any pronounced peaks. It was decided, therefore, to calculate the values of the transfer functions at frequency intervals of approximately 0.25 Hz in the range from 0 to 20 Hz, 2 Hz from 20 to 60 Hz, and 4 Hz from 60 to 120 Hz. Because the Δf required is of the order of 0.25 Hz the values of the transfer functions at intermediate points are evaluated by interpolation between the computed values. Finally, because f_{max} should be approximately 240 Hz the values between 120 and 240 Hz were obtained by extrapolation. The preliminary studies indicated that the results obtained with these simplifications (leading to considerable savings in computer time) were in good agreement with those obtained using a constant frequency increment of 0.25 Hz over the complete range of freqencies.

Figure 14 shows typical time histories of the displacements at Point 1 (center of the loaded area) and Point 7 (farthest station) for a depth to bedrock of 20 ft. From these figures the peak deflection was computed at each station and the deflection bulb was obtained. Figure 15 shows the ratio of the dynamic to the static deflections considering both a finite layer and a half-space for the static analyses. It can be seen that a small amount of dynamic amplification takes place particularly as the distance to the load increases although dynamic effects are much less pronounced than in the case of the Dynaflect.

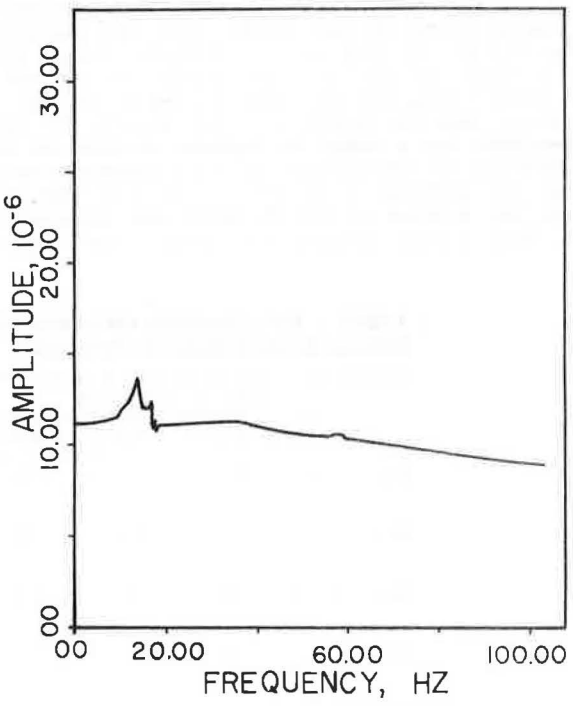

FIGURE 13 Transfer function at Point 1 (center of load) at H = 20 ft—falling weight deflectometer.

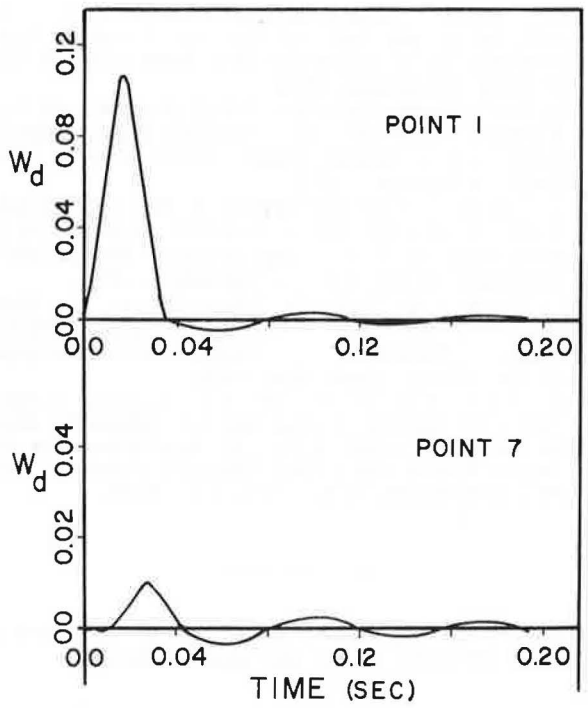

FIGURE 14 Time history of deflections at Points 1 and 7—falling weight deflectometer.

The computed deflections and the estimated moduli of the pavement, base, and subbase for the cases studied are summarized in Table 3. Although the errors are now much smaller, there are still some significant differences for shallow soil deposits (i.e., 10 ft) where the stiffness of the subbase is overestimated and for some intermediate depths (40 ft) where the modulus of the subbase is underestimated but that of the pavement is overestimated by 40 percent.

CONCLUSIONS

The results of the studies conducted to date indicate that a static interpretation of the deflections measured in the Dynaflect tests may be reasonable when dealing with a homogeneous soil (subbase) extending to depths of 60 ft or more. When much stiffer bedrock is encountered at shallower depths important dynamic amplification can occur. The elastic properties backfigured for the pavement system using standard techniques can then be substantially in error. The situation is aggravated when the soil of the subbase is not homogeneous but its stiffness increases with depth.

Dynamic effects are less important for the falling weight deflectometer because a broad range of frequencies is excited instead of a single one. Even so there are still some ranges of depth to bedrock for which the differences in dynamic effects at the various stations (distorting the shape of the de-

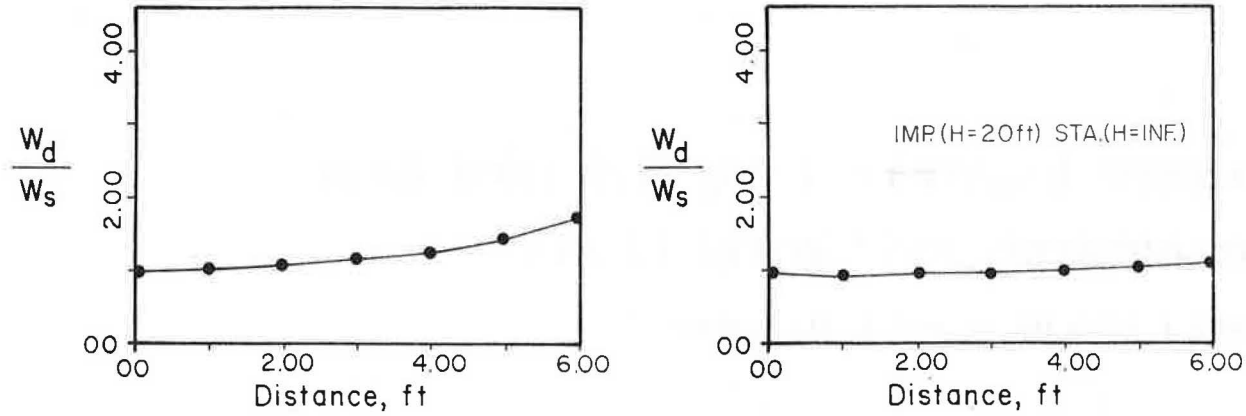

FIGURE 15 Ratio of dynamic (IMP) to static (H = ∞) deflections at H = 20 ft—falling weight deflectometer.

TABLE 3 Deflection Bulbs and Estimated Elastic Moduli for Homogeneous Subbase and Different Depths to Bedrock, Falling Weight Deflectometer (displacement x 10^{-8} ft)

		Distance to the Center (ft)								
	H (ft)	0	1	2	3	4	5	6	Estimated (lb/in^2)	Errors (%)
Static	∞	11.54	5.139	3.141	2.180	1.611	1.253	1.015	200,000	
									78,500	
									29,000	
Dynamic	10	10.60	4.622	2.842	1.923	1.317	0.9094	0.7214	200,000	
									78,500	0.0
									35,539	
Dynamic	20	11.06	4.652	3.013	2.073	1.538	1.280	1.090	200,000	0.0
									82,200	4.7
									28,790	0.7
Dynamic	40	10.74	4.860	3.008	2.111	1.590	1.288	1.086	287,200	43.6
									87,375	11.3
									28,331	2.3
Dynamic	80	11.08	4.733	3.073	2.109	1.608	1.311	1.044	200,000	0.0
									89,131	13.5
									29,245	0.8

flection bulb) may lead to erroneous estimates of the elastic moduli.

ACKNOWLEDGMENTS

The work described in this paper was conducted at The University of Texas at Austin under a research grant from the Texas State Department of Highways and Public Transportation.

REFERENCES

1. W.T. Thomson. Transmission of Elastic Waves Through a Stratified Soil Medium. Journal of Applied Physics, Vol. 21, Feb. 1950.
2. N.A. Haskell. The Dispersion of Surface Waves on Multilayered Media. Bulletin of the Seismological Society of America, Vol. 43, No. 1, Feb. 1953.
3. E. Kausel and J.M. Roesset. Stiffness Matrices for Layered Soils. Bulletin of the Seismological Society of America, Vol. 71, No. 6, Dec. 1981.
4. G. Gazetas. Dynamic Stiffness Functions of Strip and Rectangular Footings on Layered Soils. S.M. thesis. Massachusetts Institute of Technology, Cambridge, 1975.
5. R.J. Apsel. Dynamic Green's Functions for Layered Media and Applications to Boundary Value Problems. Ph.D. dissertation. University of California, San Diego, 1979.
6. G. Waas. Linear Two-Dimensional Analysis of Soil Dynamics Problems on Semi-Infinite Layered Media. Ph.D. dissertation. University of California, Berkeley, 1972.
7. E. Kausel. Forced Vibrations of Circular Foundations on Layered Media. Research Report R74-11. Department of Civil Engineering, Massachusetts Institute of Technology, Cambridge, 1974.
8. E. Kausel. An Explicit Solution for the Green Functions for Dynamic Loads in Layered Media. Research Report R81-13. Massachusetts Institute of Technology, Cambridge, 1981.
9. W. Uddin, W.R. Meyer, and K.H. Stokoe. Project-Level Structural Evaluation of Pavements Based on Dynamic Deflections. In Transportation Research Record 1007, TRB, National Research Council, Washington, D.C., 1985, pp. 37-45.

Publication of this paper sponsored by Committee on Mechanics of Earth Masses and Layered Systems.

Pavement Evaluation Using Deflection Basin Measurements and Layered Theory

ALBERT J. BUSH III and DON R. ALEXANDER

ABSTRACT

Recent developments through research efforts at the Waterways Experiment Station (WES) have produced a pavement evaluation procedure that uses deflection basin measurements from nondestructive test devices. These deflections are input for a layered elastic program (BISDEF) that predicts elastic moduli for each pavement layer for up to a four-layer system. The approach has been verified through comparison of predicted moduli from the computer program to moduli from laboratory modulus tests. The moduli determined from the deflection basin and BISDEF are then used with limiting strain criteria and a layered elastic program (AIRPAVE) to determine allowable aircraft loads, strengthening overlay requirements, and so forth. The use of a single evaluation procedure that employs test results from six different nondestructive testing devices to determine the allowable aircraft load on flexible airfield pavements is evaluated. Test data presented here were obtained from a side-by-side comparative study conducted in October 1982 at MacDill Air Force Base on three different pavements (two asphalt concrete and one composite of asphalt concrete over portland cement concrete). Test devices considered in this paper are the WES 16-kip vibrator, three falling weight deflectometers, a Road Rater, and a Dynaflect. Allowable loads determined using data from each device compare favorably with the standard evaluation procedure. The moduli values for the base course materials are higher when a preload is applied as in the case of the WES 16-kip vibrator.